Eur. J. Mineral., 36, 863–872, 2024
https://doi.org/10.5194/ejm-36-863-2024
© Author(s) 2024. This work is distributed under
the Creative Commons Attribution 4.0 License.

European Journal of Mineralogy
Open Access

Bonacinaite, $Sc(AsO_4) \cdot 2H_2O$, the first scandium arsenate

Marco E. Ciriotti[1,2], Uwe Kolitsch[3,4], Fernando Cámara[5], Pietro Vignola[6], Frédéric Hatert[7], Erica Bittarello[8], Roberto Bracco[9], and Giorgio Maria Bortolozzi[10,†]

[1]AMI – Associazione Micromineralogica Italiana, via San Pietro 55, 10073 Devesi-Cirié, Italy
[2]Dipartimento di Scienze della Terra, Università degli Studi di Torino,
via Tommaso Valperga Caluso 35, 10125 Turin, Italy
[3]Mineralogisch-Petrographische Abt., Naturhistorisches Museum, Burgring 7, 1010 Vienna, Austria
[4]Institut für Mineralogie und Kristallographie, Universität Wien, Josef-Holaubek-Platz 2, 1090 Vienna, Austria
[5]Dipartimento di Scienze della Terra "Ardito Desio", Università degli Studi di Milano,
via Luigi Mangiagalli 34, 20133 Milan, Italy
[6]CNR – Istituto di Geologia Ambientale e Geoingegneria, via Mario Bianco 9, 20131 Milan, Italy
[7]Laboratoire de Minéralogie, Université de Liège, 4000 Liège, Belgium
[8]Dipartimento di Scienze della Terra, Università degli Studi di Torino,
via Tommaso Valperga Caluso 35, 10125 Turin, Italy
[9]AMI – Associazione Micromineralogica Italiana, via Montenotte 18/6, 17100, Savona, Italy
[10]AMI – Associazione Micromineralogica Italiana, via Dogali 20, 31100 Treviso, Italy
†deceased

Correspondence: Marco E. Ciriotti (marco.ciriotti45@gmail.com)

Received: 17 May 2024 – Revised: 5 August 2024 – Accepted: 7 August 2024 – Published: 19 September 2024

Abstract. The new mineral bonacinaite (IMA2018-056), $Sc(AsO_4) \cdot 2H_2O$, was found on the dumps of the Varenche Mine (Saint-Barthélemy, Nus, Aosta Valley, Italy), an old manganese mine, where it occurs as a low-temperature hydrothermal mineral associated mainly with quartz, granular braunite, undefined manganese oxides, arseniopleite, manganberzeliite and thortveitite. Bonacinaite forms colourless (with faint to distinct violet tints), pseudohexagonal, thick tabular crystals, up to 0.25 mm in size, sometimes with annular internal zones showing violet tinges, or as small, faintly violet lath-shaped crystals. The crystals are transparent and brittle, with vitreous lustre. The calculated density of an almost pure bonacinaite crystal is 2.82 g cm^{-3}. Optically, bonacinaite is biaxial negative, $\alpha = 1.598(4)$, $\beta = 1.618(3)$, and $\gamma = 1.638(3)$ (measured with a Na light source, 589 nm); $2V$ (measured) is large, and $2V$ (calculated) $= -88.9°$. The empirical formula, based on six O atoms per formula unit is $(Sc_{0.90}Mn^{3+}_{0.08}Fe^{3+}_{0.01}Pb_{0.01})_{\Sigma 1.00}[(As_{0.95}P_{0.06})_{\Sigma 1.01}O_4] \cdot 2H_2O$. Bonacinaite has monoclinic symmetry, with space group $P2_1/n$ and unit-cell parameters (single-crystal data / powder diffraction data) $a = 5.533(1)/5.521(1)$, $b = 10.409(2)/10.336(3)$, $c = 9.036(2)/9.059(4)$ Å, $\beta = 91.94(3)/91.97(4)$, $V = 520.1(2)/516.7(3)$ Å^3 and $Z = 4$. The crystal structure was refined from single-crystal intensity data obtained from a distinctly Al- and P-bearing crystal to $R_1(F) = 3.7$ % for 1178 reflections. Bonacinaite is isotypic with the other members of the metavariscite group: kolbeckite, metavariscite and phosphosiderite.

1 Introduction

Scandium is the 23rd most abundant element in the Sun and similar stars, as well as on lunar soil, but only the 50th most abundant on Earth. It is the lightest element in the early transition series and often shows extraordinary behaviour due to the presence of empty 3d states in a trivalent state in ionic compounds. The chemical properties of scandium differ significantly from those of other transition elements, and this unique chemistry is currently being exploited for some high-performance applications. The major application is as an alloy with metals like aluminium, magnesium, zirconium, etc. These alloys find extensive use in sports, military, aircraft and spacecraft (reduction of weight, which in turn reduces the fuel consumption and, thus, CO_2 emission), solid oxide fuel cells (SOFCs), mercury vapour lamps, tracing agents in oil refineries, and nuclear medicine (Borgese, 1993; Sabatini et al., 2017; Siegfried et al., 2018).

In the Earth's crust scandium is widely distributed, and more than 800 minerals normally contain traces of scandium. Frondel (1968) and Foord et al. (1993) concluded that "scandium in the ferromagnesian minerals apparently substitutes for iron in sites occupied by either (Fe^{3+},Al) or (Fe^{3+},Mg). Scandium can also form limited solid solution with Y^{3+}, Al, the heavy lanthanides, Ti^{4+}, Sn^{4+}, Zr^{4+} and W^{6+} in certain geochemical environments". They also concluded that "discoveries of new scandium minerals may be expected in the years to come, as we know that Sc^{3+} may substitute for Fe^{3+} – Al^{3+} in pyroxenes and amphiboles in Sc-rich environment". However, presently only 22 minerals with Sc as an essential element are recognised as valid species by the IMA Commission on New Minerals, Nomenclature and Classification (CNMNC), and 5 (22.7 %) of these are found only in meteorites as refractory phases among the very first solids forming in the solar system. Eleven Sc minerals are silicates, six are oxides and four are phosphates. Among the latter, kolbeckite, $Sc^{3+}(PO_4) \cdot 2H_2O$, has a high scandium content but does not occur in any larger deposits.

Bonacinaite, $Sc^{3+}(AsO_4) \cdot 2H_2O$ (pronunciation: bo-na-chee-na-ait; Russian БОНАЦИНАИТ; abbreviation Bci; Warr, 2021) is a new mineral species approved by the CNMNC (IMA2018-056) and the first known Sc-arsenate mineral. It was found on the dumps of the abandoned Varenche Mine (45°47′25″ N, 7°28′55″ E), Les Fabriques, Saint-Barthélemy, Nus, in the Italian region of Valle d'Aosta (Aosta Valley) (Barresi et al., 2005, 2007a; Cámara et al., 2018); no other occurrence is currently known.

The name honours Enrico Bonacina (1928–2024), the "dean" photographer of microminerals in Italy (and perhaps in Europe), known everywhere in this field by collectors as "Maestro Bonacina". Mr. Bonacina was a passionate student of biology, astronomy and sciences in general and a researcher and collector of minerals, who co-authored papers on systematic and regional mineralogy. In the early 1970s, dissatisfied with the results of mineral photography with microscopes through the tools of that time, and thanks to his personal work experience in optical lenses, he built special equipment with which he obtained excellent results. From then on, he never stopped providing tens of thousands of photographs to magazines, collector friends, university professors and researchers, who were able to take advantage of excellent photographic documentation (which naturally had a qualitative turnaround with the advent of digital microphotography), always free of charge.

The naming aims, at the same time, to valorise and highlight the important contribution of mineral photographers to systematic and descriptive mineralogy.

The type material, which comprises a probe mount and a rock chip, is deposited in the Mineralogical Collection of the Museum of the Earth Sciences Department of the University of Milan, Italy (catalogue number MCMGPG-H2018-001). The crystal used for the crystal-structure determination and a micromount-sized specimen with a few tiny crystals are deposited in the collection of the Natural History Museum, Vienna, Austria (catalogue number O 571). The crystal used for optical measurements is mounted on a spindle stage and deposited in the Mineralogical Collection of the Laboratory of Mineralogy, University of Liège, Belgium (catalogue number 21180).

2 Occurrences

The mineral, first found in 2005 by two of the authors (Giorgio Maria Bortolozzi and Marco E. Ciriotti) in almost colourless (with faint violet tints), tabular, pseudohexagonal micro-crystals, was preliminarily identified as a potential new species by SEM-EDS and micro-Raman analysis through the AMI (Associazione Micromineralogica Italiana) unknown service identification (Marco E. Ciriotti and Roberto Bracco), and nearly all crystals found were subsequently used for the complete characterisation of bonacinaite. A few specimens were also found inside the dumps by one of the authors (Roberto Bracco). In later times, some stockier, purple-blue crystals of bonacinaite were found by the skilled field collector Francesco Vanini.

Bonacinaite occurs very rarely (about a dozen samples in total) in the dumps of the Varenche Mine, an abandoned old manganese mine (45°47′25″ N, 7°28′55″ E) in the valley (*vallone*) of Saint-Barthélemy (orographic right of the homonymous stream), Nus, Aosta Valley, Italy. The mine is close to the better-known manganese Prabornaz Mine, on the opposite side of the river Dora Baltea, in the Saint-Marcel valley.

The Varenche Mine consists of (1) an upper tunnel, approximately 2 km long, the only one from which quartz-rich manganese ore was extracted during the mine's period of activity (from 1415 to the early 1900s) and sent to the glass industry to be used as a bleaching agent; (2) a mineralogically sterile lower tunnel, less than 100 m long; and (3) dumps to

the right and left (Fig. 1) of the first ∼250 m of the footpath, which reaches the hamlet of Lignan in about 30 min. Presently, all tunnels are closed by gates.

Pelloux (1922) reported that the deposit was composed of a bank of jasper, with a maximum thickness of about 2 m, in which manganese ore layers and lenses were interleaved: shiny black braunite, smaller quantities of spessartine, piemontite, rhodochrosite, Mn-bearing siderite, "ardennite" and "alurgite" (a Mn^{3+}-bearing red-pink variety of muscovite-2M_1). The exploited ore formed a bench about 1 m thick and consisted of braunite, spotted by spessartine stains and thin veins. It is associated with quartzites belonging to the calc-schist and the greenstone assemblage of the Piedmont complex of the Western Alps. The ore formed in a submarine environment by exhalative hydrothermal activity related to ophiolitic volcanism and subsequently was recrystallised and deformed during the Alpine orogeny. Baldelli et al. (1983) report evidence of Alpine metamorphism in the ore-bearing quartzites of Varenche, with some relics of high-pressure metamorphism in a dominant context of low-grade equilibration.

Barresi et al. (2005) report up to 61 mineral species in the dumps of the Varenche Mine. They also report the identification, by means of SEM-EDS data and a crystal-structure refinement, of an unnamed scandium arsenate analogue of metavariscite (= bonacinaite) which forms very small (0.05–0.25 mm) transparent, pseudohexagonal crystals with a violet tint in a small void with associated braunite, quartz, albite and corroded crystal aggregates of arsenioplеite. Minerals associated with bonacinaite within the void itself are quartz, granular braunite, undefined manganese oxides, arsenioplеite, manganberzeliite and thortveitite.

The Varenche Mine is also the source of further rare and scientifically interesting mineral species. Bonazzi et al. (1996) identified an intermediate member of the piemontite–androsite series that suggests the existence of a continuous solid solution between the two minerals, including the later approved manganiandrosite-(Ce). Barresi et al. (2007b) recognised the occurrence of ardennite-(V), previously studied by Pasero et al. (1994). Oberti et al. (2017) worked on a specimen from the Varenche Mine for the crystal–chemical characterisation of the grandfathered end-member magnesio-riebeckite, and Bonino et al. (2023) document the occurrences of the two manganese oxalate hydrates falottaite and lindbergite. Currently (2024), the total number of valid mineral species found in the Varenche Mine dumps is 75.

3 Appearance and properties

Bonacinaite occurs as colourless (with faint to distinct violet tints, attributed to trace contents of Mn^{3+}), pseudohexagonal, thick tabular, transparent crystals, up to 0.25 mm in size (Barresi et al., 2005), sometimes with annular internal zones showing violet tints or as small faintly violet laths (Figs. 2–3). The crystals show a vitreous lustre and are brittle. Only about a dozen small specimens, each with a very small (max. 10) number of crystals, are known.

The habit of bonacinaite crystals is either thick tabular, pseudohexagonal or lath-shaped, with forms {001}, {010} and {110}. The pseudohexagonal crystal used for the structure determination is thick tabular on {001} according to indexing on a single-crystal diffractometer; a combination of (010) and $(0\bar{1}0)$ with (110), $(\bar{1}10)$, $(\bar{1}\bar{1}0)$ and $(1\bar{1}0)$ produces the pseudohexagonal outline (Fig. 3). Twinning was not observed. The $a:b:c$ ratio calculated from the single-crystal unit-cell parameters is $0.532:1:0.874$.

Optically, bonacinaite is biaxial negative, $\alpha = 1.598(4)$, $\beta = 1.618(3)$, and $\gamma = 1.638(3)$ (measured with a Na light source, 589 nm); $2V$ (measured) is large, and $2V$ (calculated) $= -88.9°$. We could not observe a suitable interference figure, but considering the agreement with chemistry (see Gladstone–Dale compatibility index below) we rely on the refraction index measurements. The mineral is pleochroic, X is colourless to light grey, Y is light violet and Z is light violet. Dispersion was not observed. The optical orientation could not be determined.

The streak is white, and no fluorescence, in either short-wave (254 nm) or long-wave (366 nm) ultraviolet light, was observed. Cleavage, parting and fracture were not observed. Mohs hardness was not measured; by analogy with other members of the metavariscite group it is estimated to be in the range 3.5–4.

The density was not measured due to size, scarcity and close association with other mineral phases, but it was calculated as $2.82\,g\,cm^{-3}$ using the empirical formula and $2.63\,g\,cm^{-3}$ from the single-crystal structure refinement of an Al- and P-bearing crystal, $(Sc_{0.807}Al_{0.193})(As_{0.767}P_{0.233})O_4 \cdot 2H_2O$ (specimen O 571).

4 Chemical composition

Quantitative chemical analysis (eight points) was done with a Jeol JXA-8200 electron probe microanalyser, at the Earth Science Department of the University of Milan (ESD-UMI) (WDS mode, 15 kV, 5 nA, 5 µm beam diameter). F and S were analysed but found to be below detection limits. EDS spectra showed the absence of any further element heavier than Na. The presence of H_2O was confirmed by Raman spectroscopy and the crystal-structure determination. Analytical results are given in Table 1.

The mineral grain analysed showed high beam sensitivity and high porosity that yielded low totals, although stoichiometry is in perfect agreement with the crystal-structure data. The empirical formula (based on 6 O atoms pfu) is $(Sc_{0.90}Mn^{3+}_{0.08}Fe^{3+}_{0.01}Pb_{0.01})_{\Sigma 1.00}[(As_{0.95}P_{0.06})_{\Sigma 1.01}O_4] \cdot 2H_2O$. The ideal formula is $Sc(AsO_4) \cdot 2H_2O$, which requires (wt %) Sc_2O_3 31.45, As_2O_5 52.20, and H_2O 16.35,

Figure 1. Partial view of the dump of the Varenche Mine, November 2014. Picture: Franco Luca Bonino.

Table 1. Chemical–analytical data (wt %) for bonacinaite.

Constituent	Mean	Range	SD	Normalised	Probe standard
As_2O_5	44.24	42.69–45.19	0.81	49.37	Realgar
P_2O_5	1.59	1.34–1.94	0.27	1.78	Synthetic YPO_4
Sc_2O_3	25.04	24.27–25.82	0.48	27.94	Synthetic $ScPO_4$
Fe_2O_3	0.25	0.08–0.54	0.14	0.28	Fayalite
Mn_2O_3	2.53	1.87–3.89	0.65	2.82	Rhodonite
PbO	1.36	1.10–1.60	0.20	1.51	Galena
K_2O[a]	0.77	0.45–1.12	0.23		K-feldspar
H_2O[b]	14.60	14.20–14.85	0.21	16.29	
Total	89.60	86.71–90.52	1.31	100.00	

[a] K_2O content is a K-feldspar contamination. [b] Assuming $2H_2O$ per formula unit (pfu).

with a total of 100.00. The Gladstone–Dale compatibility 1 − (Kp/Kc) equals 0.013 (superior).

5 X-ray diffraction and crystal structure

A euhedral single crystal of bonacinaite ($0.06 \times 0.07 \times 0.10$ mm; Fig. 3), with uniform extinction and free of inclusions under a transmitted-light polarising microscope, was used. A full sphere of X-ray diffraction intensity data up to $2\theta = 60.22°$ was collected at room temperature at the Institut für Mineralogie und Kristallographie, Universität Wien, with a Nonius KappaCCD single-crystal X-ray diffractometer equipped with a CCD area detector and using monochromatised Mo-$K\alpha$ radiation (50 kV, 30 mA). Standard processing ($R_{int} = 0.0243$) gave the following crystal data: monoclinic, space group $P2_1/n$, $a = 5.533(1)$, $b = 10.409(2)$, $c = 9.036(2)$ Å, $\beta = 91.94(3)$, $V = 520.1(2)$ Å^3 and $Z = 4$. The structure was refined to $R_1 = 0.0367$ on the basis of 1178 unique reflections [$F > 4\sigma(F)$] out of a total of 1470. The atomic arrangement of bonacinaite is constituted of $ScO_4(H_2O)_2$ octahedra linked through (AsO_4) tetrahedra into a three-dimensional

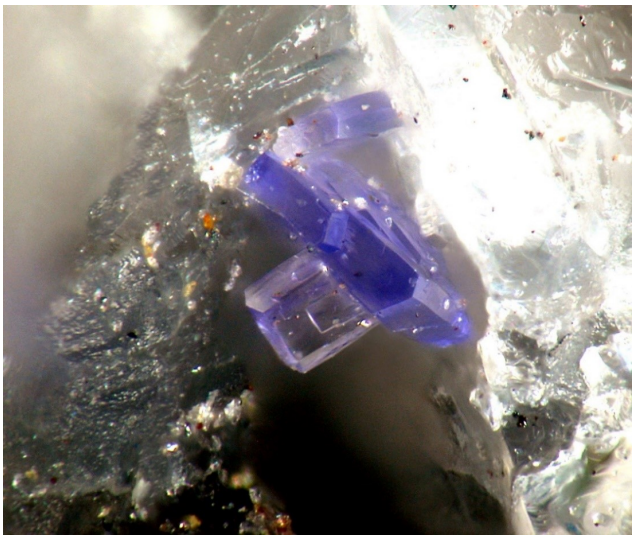

Figure 2. Bonacinaite as a group of two lath-shaped light violet and eight dark purple-blue crystals in a very small void of a quartz–braunite matrix. Field of view: 0.3 mm. Picture: Giorgio Maria Bortolozzi.

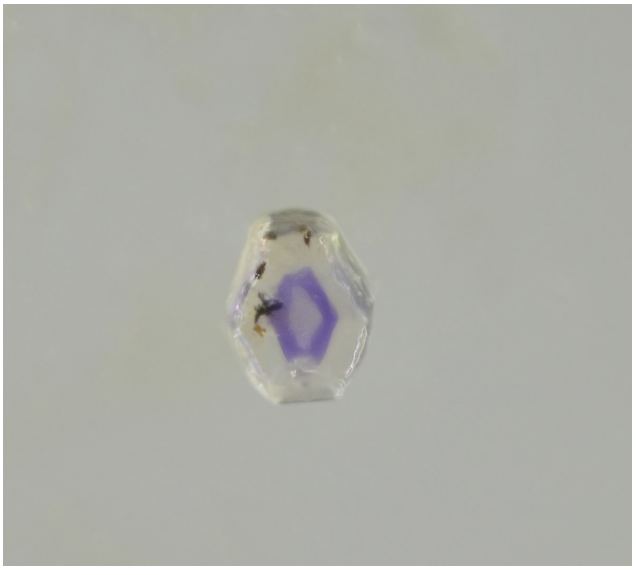

Figure 3. Thick tabular, pseudohexagonal bonacinaite crystal ($0.06 \times 0.07 \times 0.10$ mm; used for the crystal-structure determination; catalogue number O 571) with a violet annular zone (a pale-yellow tint is due to high-vacuum grease coating the crystal's surface). Picture: Harald Schillhammer.

framework (Fig. 4). Hydrogen atoms bonded to H_2O groups show strong hydrogen bonding (O–H···O = 2.64–2.81 Å). Further details of the crystal structure of bonacinaite were already discussed in Kolitsch et al. (2020), including a comparison with other natural and synthetic members of the metavariscite and variscite groups.

Table 2. X-ray powder diffraction data for bonacinaite.

$I_{obs.}$	$d_{obs.}$ (Å)	$I_{calc.}$	$d_{calc.}$ (Å)	*hkl*
15	6.812	33	6.821	0 1 1
11	5.171	36	5.205	0 2 0
100	4.865	90	4.883	1 1 0
		7	4.789	1 0 $\bar{1}$
18	4.638	18	4.646	1 0 1
32	4.525	100	4.515	0 0 2
		16	4.509	0 2 1
8	4.341	15	4.350	1 1 $\bar{1}$
33	3.771	44	3.790	1 2 0
		12	3.366	1 1 $\bar{2}$
43	2.924	65	2.939	1 2 $\bar{2}$
		32	2.939	1 3 0
16	2.862	30	2.891	0 1 3
		22	2.870	1 2 2
3	2.800	6	2.810	1 3 $\bar{1}$
31	2.759	9	2.780	1 3 1
94	2.665	22	2.682	1 0 $\bar{3}$
		26	2.672	2 1 0
8	2.609	10	2.607	1 0 3
		6	2.606	0 2 3
6	2.580			2 1 1
16	2.534	7	2.540	2 1 1
5	2.479	8	2.484	1 3 $\bar{2}$
4	2.435	6	2.443	1 3 2
3	2.391	6	2.394	2 0 $\bar{2}$
8	2.333	5	2.355	1 0 4
		5	2.340	2 2 1
7	2.266	8	2.273	0 3 3
3	2.118	6	2.122	1 3 $\bar{3}$
7	1.866	8	1.869	2 2 3
3	1.785	5	1.789	2 2 $\bar{3}$
36	1.733	13	1.737	3 2 0
		8	1.734	1 0 $\bar{5}$
4	1.655	6	1.663	2 5 0
3	1.431	5	1.431	2 2 5

X-ray powder diffraction data were obtained from a multiple grain. The dataset was collected at the XRD1 beamline at the Elettra synchrotron radiation facility, Basovizza, Trieste, Italy, using a wavelength of $\lambda = 0.68880$ Å and a PILATUS 2M area detector. Observed interplanar spacings and intensities of indexed reflections using Highscore (Degen et al., 2014) and $d(I)$ values calculated using Vesta (Momma and Izumi, 2011) are reported in Table 2. Unit-cell parameters refined using GSAS (Larson and Von Dreele, 1994) are as follows: $a = 5.521(1)$, $b = 10.336(3)$, $c = 9.059(4)$ Å, $\beta = 91.97(4)$ and $V = 516.7(3)$ Å^3.

6 Raman spectroscopy

The micro-Raman spectrum of bonacinaite was obtained at the Dipartimento di Scienze della Terra (Università degli

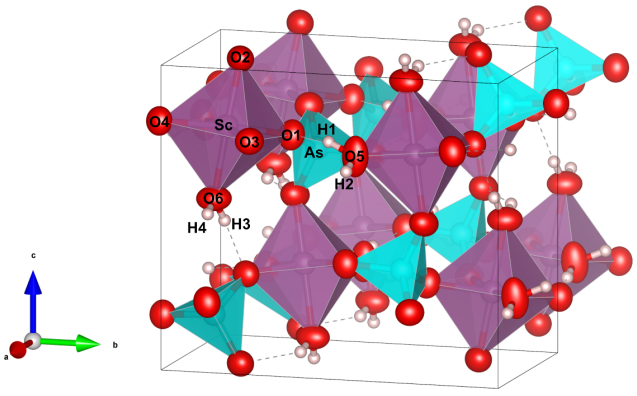

Figure 4. Polyhedral representation of the crystal structure of bonacinaite: violet – Sc, green – As, red – oxygen and grey – hydrogen. Displacement ellipsoids are drawn at the 80 % probability level. Hydrogen bonds are shown as dashed grey lines. Figure drawn with Vesta 3.0 (Momma and Izumi, 2011).

Studi di Torino) using a micro/macro Jobin Yvon LabRam HRVIS, equipped with a motorised x–y stage and an Olympus microscope. The backscattered Raman signal was collected with a 50× objective, and the spectrum was obtained from a randomly oriented crystal. The 632.8 nm line of a He–Ne laser was used as excitation; laser power was controlled by means of a series of density filters. The minimum lateral and depth resolution was set to a few micrometres. The system was calibrated using the 520.6 cm^{-1} Raman band of silicon before each experimental session. Spectra were collected with multiple acquisitions (two to six) with single counting times ranging between 20 and 180 s. The spectra were recorded from 200 to 4000 cm^{-1} using the LabSpec 5 program (Fig. 5).

Comparing the Raman spectrum of bonacinaite with the spectra of other members of the metavariscite group (Kloprogge and Wood, 2017; see also Knops-Gerrits et al., 2000; Frost et al., 2004; Sergeeva, 2016; Fritsch et al., 2017), the spectrum shows a strong band at 912 cm^{-1} that can be interpreted as the asymmetric stretching vibration of the arsenate anion. There is another strong band at 834 cm^{-1}, with a shoulder at 844 cm^{-1} (arsenate symmetric stretching mode), a band at 441 cm^{-1} (antisymmetric bending υ_4 of AsO_4), and a lower-intensity band at 363 and 327 cm^{-1} (symmetric bending υ_2 of AsO_4). Lattice modes are present in the range below 320 cm^{-1} (311 and 174 cm^{-1}), which have also been observed in scorodite (Kloprogge and Wood, 2017). A weak band at around 1009 cm^{-1} can be interpreted as the antisymmetric stretching mode $\upsilon_3(F_2)$ of PO_4 groups, which are present in a low amount (see Table 1). At around 1651 cm^{-1} a weak band shows the presence of H_2O groups (H_2O bending modes). A broad band composed of three peaks at ∼3000, ∼3079 and ∼3200 cm^{-1} corresponds to the OH stretching mode in H_2O groups, with similar values observed in Raman spectra of scorodite at 3080–3082 cm^{-1} (Kloprogge and Wood, 2017). The sharp band at 3513–3575 cm^{-1} observed in scorodite, mansfieldite, variscite and phosphosiderite (Kloprogge and Wood, 2017) has not been observed and probably indicates that in bonacinaite all the H atoms are involved in shorter H···O interactions; however, an orientation effect cannot be excluded.

7 Discussion

7.1 Origin of bonacinaite

In the Varenche deposit the arsenosilicate ardennite-(As), the vanadosilicate ardennite-(V), and the arsenates arseniopleite, conichalcite, manganberzeliite, sarkinite, tilasite and wallkilldellite are not so rare, while the only identified phosphates are the uncommon hydroxylapatite and pyromorphite. The presence of scandium in the deposit is reflected by the localised occurrence of a fair amount of blue thortveitite, closely associated with arseniopleite, in a small, very dangerous (collapsed roof and walls) humid section of the upper tunnel, difficult to reach without adequate equipment. In contrast, thortveitite is rare in the dump. Evidently, the smallness of the thortveitite-containing area in the tunnel is the reason that thortveitite and arseniopleite are only rarely found in the dump, as is the even rarer bonacinaite.

Tentatively, we can infer that bonacinaite is a low-temperature hydrothermal phase whose primary sources of Sc and As may have been thortveitite and arseniopleite and/or manganberzeliite, respectively, which are typically associated with it.

7.2 Relation to other species and the metavariscite group

Bonacinaite is identical to UM2005-02-AsO:AlHMgPScSi in the system of codification for unnamed minerals (Smith and Nickel, 2007) and updated IMA lists (2023) of unnamed minerals; this phase was first described as the unnamed As analogue of metavariscite from the Varenche Mine (Barresi et al., 2005). Bonacinaite represents the As analogue of kolbeckite ($ScPO_4 \cdot 2H_2O$) and, along with phosphosiderite ($Fe^{3+}PO_4 \cdot 2H_2O$), belongs to the metavariscite ($AlPO_4 \cdot 2H_2O$) group. Synthetic metavariscite-type compounds, currently unknown as minerals, are $VPO_4 \cdot 2H_2O$ (Schindler et al., 1995), $GaPO_4 \cdot 2H_2O$ (Mooney-Slater, 1961, 1966) and $InPO_4 \cdot 2H_2O$ (Sugiyama et al., 1999; Tang et al., 2002). No metal(II) selenate representatives are known, unlike the situation in the variscite group (Kolitsch et al., 2020).

The crystal structure of bonacinaite is related to that of the variscite group (orthorhombic, space group *Pbca*), which comprises the phosphates variscite ($AlPO_4 \cdot 2H_2O$) and strengite ($Fe^{3+}PO_4 \cdot 2H_2O$) and the arsenates mansfieldite ($AlAsO_4 \cdot 2H_2O$), scorodite ($Fe^{3+}AsO_4 \cdot 2H_2O$) and yanomamite ($In^{3+}AsO_4 \cdot 2H_2O$). Synthetic arsenate repre-

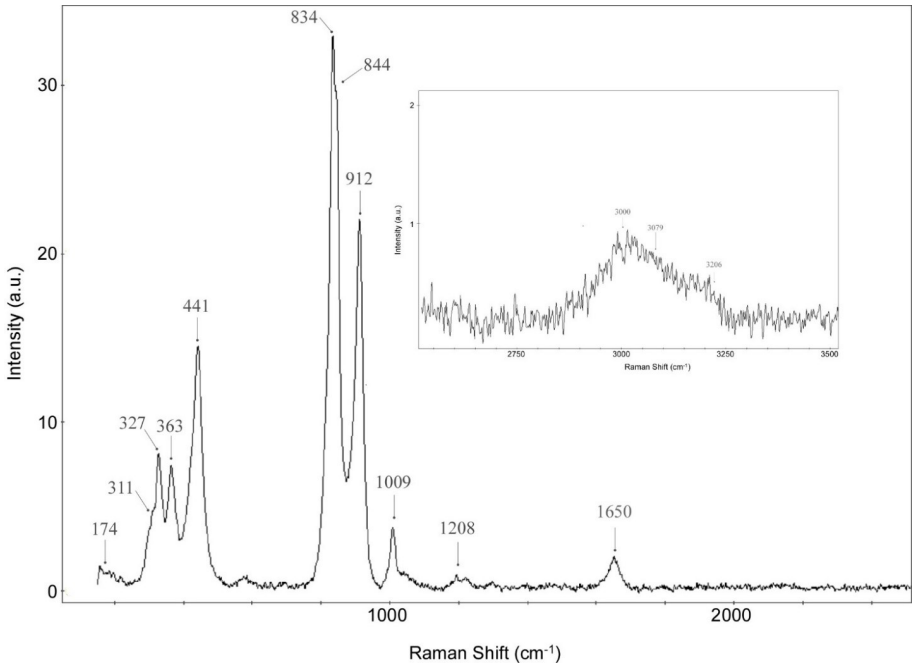

Figure 5. Bonacinaite micro-Raman spectrum in the range 100–2500 cm^{-1}. In the top right box, the range 2000–3500 cm^{-1} is shown.

sentatives are $GaAsO_4 \cdot 2H_2O$ (Dick, 1997; Le Berre et al., 2007; Spencer et al., 2015) and $Tl^{3+}AsO_4 \cdot 2H_2O$, as well as $Cr^{3+}AsO_4 \cdot 2H_2O$ (Kolitsch et al., 2020). The structural relationship between the two groups of compounds has been discussed by Moore (1966), Loiseau et al. (1998), Taxer and Bartl (2004), and Kolitsch et al. (2020).

Bonacinaite is the first scandium arsenate mineral with metavariscite structure. As observed for other members of the metavariscite group, bonacinaite shows somewhat high equivalent displacement parameters for the O5 site, displaying a probable slight positional disorder of this H_2O group, an observation which might be explained by the mixed occupancy of the octahedrally and tetrahedrally coordinated sites (Al- and P-bearing specimen O 571).

Although bonacinaite has long been known as a synthetic compound (Carron et al., 1958; Ivanov-Emin et al., 1971; Komissarova et al., 1971, 1973), its crystal structure had never been determined. Komissarova et al. (1971) reported a pseudo-orthorhombic unit cell with $a = 5.64(5)$, $b = 10.47(1)$, $c = 9.36(1)$ Å, $\beta \sim 90$ and $V \sim 553$ Å^3, which roughly agrees with our data, although, as expected, these unit-cell parameters are larger than those of the Al- and P-bearing specimen O 571.

The hexagonal ($P3_1c$) parascorodite ($Fe^{3+}AsO_4 \cdot 2H_2O$) also has some crystal–chemical relation to bonacinaite, although the structure topology is completely different.

7.3 Metavariscite group

The metavariscite group includes isotypic monoclinic arsenates and phosphates with the general formula $AXO_4 \cdot 2H_2O$, where A denotes a trivalent cation (Sc^{3+}, Fe^{3+}, Al^{3+}, In^{3+}, Ga^{3+}) and X is P^{5+} or As^{5+}. Each PO_4 or AsO_4 tetrahedron shares four vertices with four $AO_4(H_2O)_2$ octahedra and vice versa, forming a three-dimensional network of polyhedra. A possible disordered distribution of the water molecule in the channel along the c axis is suggested by literature data. The phosphate members are also dimorphous with the corresponding phosphate members of the orthorhombic (*Pbca*) variscite group. The crystal chemistry of metavariscite-type materials has been largely investigated for the biological and geochemical importance of phosphorous and arsenic, and studies have revealed interesting microporous and absorption properties (Tang et al., 2002; Huang and Shenker, 2004; O'Day, 2006; Sergeeva, 2016).

The phosphate analogue of bonacinaite and kolbeckite, ideally $Sc^{3+}(PO_4) \cdot 2H_2O$ (Edelmann, 1926; Bull et al., 2003; Yang et al., 2007), previously called "eggonite" and "sterrettite", is a rare secondary mineral of phosphate deposits and some hydrothermal veins.

Phosphosiderite, $Fe^{3+}(PO_4) \cdot 2H_2O$ (Bruhns and Busz, 1890; Moore, 1966; Fanfani and Zanazzi, 1966; Song et al., 2002; Taxer and Bart, 2004), previously named "clinobarrandite", "clinostrengite" and "metastrengite", is an alteration product of triphylite and/or similar compounds in granitic pegmatites and a replacement of bones and shells in soils. It is isotypic with kolbeckite and metavariscite and represents the monoclinic ($P2_1/n$) dimorph of orthorhombic strengite

Table 3. Comparison of miscellaneous data for bonacinaite and the other metavariscite-group minerals.

Mineral	Bonacinaite	Kolbeckite	Phosphosiderite	Metavariscite
Ideal formula	$Sc^{3+}(AsO_4) \cdot 2H_2O$	$Sc^{3+}(PO_4) \cdot 2H_2O$	$Fe^{3+}(PO_4) \cdot 2H_2O$	$Al^{3+}(PO_4) \cdot 2H_2O$
Space group	$P2_1/n$	$P2_1/n$	$P2_1/n$	$P2_1/n$
a (Å)	5.533(1)	5.4258(4)	5.30	5.178(2)
b	10.409(2)	10.2027(8)	9.77	9.514(2)
c	9.306(2)	8.9074(7)	8.73	8.454(2)
β (°)	91.94(3)	90.502(5)	90.36	90.35(2)
Z	4	4	4	4
$D_{calc.}$ (g cm^{-3})	2.82	2.35	2.72	2.535
Strongest reflections	4.865 (100)	5.100 (30)	4.912 (35)	6.325 (25)
in the X-ray powder	4.525 (32)	4.780 (100)	4.689 (100)	4.758 (100)
diffraction data,	3.771 (34)	4.440 (100)	4.363 (75)	4.552 (75)
d in Å (I)	2.924 (44)	3.708 (40)	3.610 (50)	4.227 (65)
	2.759 (31)	2.878 (70)	2.787 (85)	3.503 (60)
	2.665 (94)	2.849 (50)	2.572 (40)	2.705 (95)
Optical class, sign	biaxial (−)	biaxial (−)	biaxial (−)	biaxial (+)
α (590 nm)	1.598(4)	1.574	1.692–1.703	1.551
β	1.618(3)	1.590	1.725–1.728	1.558
γ	1.638(3)	1.600	1.738–1.739	1.582
$2V_{meas}$ (°)	large	60(10)	62–66	55
$2V_{calc}$ (°)	88.9	76	63.2–66.3	57.5
Reference	This study	Yang et al. (2004)[a]	Moore (1966)[b]	Kniep and Mootz (1973)

[a] See also Bull et al. (2003). [b] See also Fanfani and Zanazzi (1966) and Song et al. (2002).

(*Pbca*), which is isotypic with the more common arsenate scorodite ($FeAsO_4 \cdot 2H_2O$). As-bearing phosphosiderite is known as both synthetic and natural phases (e.g. 3 wt %–9 wt % As_2O_5 from Atacama, Chile; Gritsenko et al., 2022).

Metavariscite, $Al(PO_4)$ wt %$2H_2O$ (Larsen and Schaller, 1925; Borensztajn, 1966; Kniep and Mootz, 1973), previously known as "peganite", is a non-common phase in phosphate-rich veins in sedimentary phosphates and guano deposits. It is isotypic with kolbeckite and phosphosiderite and represents the monoclinic dimorph of variscite-1*O* and -2*O* (Ardit et al., 2022). Zoned phosphosiderite–metavariscite crystals were recorded in a phosphate-rich granitic pegmatite at Mina do Eduardo, Conselheiro Pena, Minas Gerais, Brazil (Lamoso and Atencio, 2017).

Comparative data for bonacinaite, kolbeckite, phosphosiderite and metavariscite are listed in Table 3.

Data availability. Crystallographic data for bonacinaite and its PXRD pattern are available in the Supplement of Kolitsch et al. (2020) at https://doi.org/10.1180/mgm.2020.57.

Author contributions. MEC conceptualised the project. FC collected powder X-ray diffraction data. WDS data were obtained by FC and PV. UK collected single-crystal X-ray diffraction data and refined them; PV and FH collected optical data and GMB contributed with a mineral specimen. UK also determined the crystal faces. MEC, RB and EB obtained the preliminary SEM-EDS analysis. EB and MEC obtained the micro-Raman spectrum. All authors processed the data and interpreted the results. The manuscript was written by MEC with contributions from all co-authors.

Competing interests. The contact author has declared that none of the authors has any competing interests.

Disclaimer. Publisher's note: Copernicus Publications remains neutral with regard to jurisdictional claims made in the text, published maps, institutional affiliations, or any other geographical representation in this paper. While Copernicus Publications makes every effort to include appropriate place names, the final responsibility lies with the authors.

Special issue statement. This article is part of the special issue "Celebrating the outstanding contribution of Paola Bonazzi to mineralogy". It is not associated with a conference.

Acknowledgements. The article benefited from constructive reviews by Ian E. Grey and Anthony R. Kampf. The manuscript was also improved by the editorial efforts and constructive comments of associate editors Elisabetta Rampone, Luca Bindi and Sergey V. Krivovichev. Franco Luca Bonino and Harald Schillhammer are thanked for providing colour photographs. The authors thank Alessandro Pavese for facilitating the WDS analyses at the University of Milan.

Financial support. This research was financially supported by Marco E. Ciriotti. Fernando Cámara received financial support from the Italian Ministry of University and Research (MUR) through the project "Dipartimenti di Eccellenza 2023–2027" and the grant Ricerca Locale 2023, Università di Milano.

Review statement. This paper was edited by Luca Bindi and reviewed by Ian Grey and Anthony Kampf.

References

Ardit, M., Phillips, B. L., and Bish, D. L.: Crystal structure determination of orthorhombic variscite *2O* and its derivative $AlPO_4$ structure at high temperature, Am. Mineral., 107, 1385–1395, 2022.

Baldelli, C., Dal Piaz, G. V., and Polino, R.: Le quarziti a manganese e cromo di Varenche-St. Barthélemy, una sequenza di copertura oceanica della falda piemontese, Ofioliti, 8, 207–221, 1983 (in Italian).

Barresi, A. A., Kolitsch, U., Ciriotti, M. E., Ambrino, P., Bracco, R., and Bonacina, E.: La miniera di manganese di Varenche (Aosta, Italia Nord-Occidentale): ardennite, arseniopleite, manganberzeliite, pirofanite, sarkinite, sursassite, thortveithite, nuovo As-Sc-analogo della metavariscite e altre specie, Micro, 3, 81–122, 2005 (in Italian with English, French and German abstracts).

Barresi, A. A., Kolitsch, U., Ciriotti, M. E., Ambrino, P., Bracco, R., and Bonacina, E.: Errata corrige: Varenche, Micro, 5, 180, 2007a (in Italian).

Barresi, A. A., Orlandi, P., and Pasero, M.: History of ardennite and the new mineral ardennite-(V), Eur. J. Mineral., 19, 581–587, https://doi.org/10.1127/0935-1221/2007/0019-1745, 2007b.

Bonazzi, P., Menchetti, S., and Reinecke, T.: Solid solution between piemontite and androsite-(La), a new mineral of the epidote group from Andros Island, Greece, Am. Mineral., 81, 735–742, 1996.

Bonino, F. L., Bittarello, E., Costa, E., and Ciriotti, M. E.: Nuovi minerali per la sistematica della miniera di Varenche (Valle d'Aosta): prima segnalazione italiana di falottaite, Micro, 21, 315–323, 2023 (in Italian with English, French and German abstracts).

Borensztajn, J.: Structures cristallines de métavariscite et de la métastrengite, B. Soc. Fr. Minéral. Cr., 89, 428–438, 1966 (in French).

Borgese, F.: Gli elementi della tavola periodica. Rinvenimento, proprietà, usi. Prontuario chimico, fisico, geologico, CISU, Roma, 254 pp., 1993 (in Italian).

Bruhns, W. and Busz, K. H. E. G.: Phosphosiderit, ein neues Mineral von der Grube Kalterborn bei Eiserfeld im Siegenschen, Z. Kristallogr., 17, 555–560, 1890 (in German).

Bull, I., Young, V., Teat, S. J., Peng, L., Grey, C. P., and Parise, J. B.: Hydrothermal synthesis and structural characterization of four scandium phosphate frameworks, Chem. Mater., 15, 3818–3825, 2003

Cámara, F., Ciriotti, M. E., Kolitsch, U., Vignola, P., Hatert, F., Bittarello, E., Bracco, R., and Bortolozzi, G. M.: Bonacinaite, IMA 2018-056, CNMNC Newsletter No. 45, October 2018, p. 1228, Mineral. Mag., 82, 1225–1232, 2018.

Carron, M. K., Mrose, M. E., and Murata, K. J.: Relation of ionic radius to structures of rare-earth phosphates, arsenates, and vanadates, Am. Mineral., 43, 985–989, 1958.

Degen, T., Sadki, M., Bron, E., König, U., and Nénert, G.: The HighScore suite, Powder Diffr., 29, S13–S18, 2014.

Dick, S.: Die Struktur von $GaAsO_4 \cdot 2H_2O$: Ein neues Mitglied der Variscit-Familie, Z. Naturforsch., B52, 1337–1340, 1997 (in German).

Edelmann, F.: Kolbeckit, ein neues sächsisches Mineral, Jahrbuch für das Berg- und Hüttenwesen im Sachsen, 100, 23–74, 1926 (in German).

Fanfani, L. and Zanazzi, P. F.: Crystalline structure of metastrengite, Atti della Reale Accademia dei Lincei, Memorie della Classe di scienze fisiche, matematiche e naturali, Rendiconti, 40, 880–889, 1966 (in Italian).

Foord, E. E., Birmingham, S. D., Demartin, F., Pilati, T., Gramaccioli, C. M., and Lichte, F. E.: Thortveitite and associated Sc-bearing minerals from Ravalli County, Montana, Can. Mineral., 31, 337–346, 1993.

Fritsch, E., Karampelas, S., and Mevellec, J.-Y.: Raman spectra of gem-quality variscite and metavariscite, J. Raman Spectrosc., 48, 1554–1558, 2017.

Frondel, C.: Crystal chemistry of scandium as a trace element in mineral, Z. Kristallogr., 127, 121–138, 1968.

Frost, R. L., Weier, M. L., Erickson, K. L., Carmody, O., and Mills, S. J.: Raman spectroscopy of phosphates of the variscite mineral group, J. Raman Spectrosc., 35, 1047–1055, 2004.

Gritsenko, Y. D., Vigasina, M. F., Dedushenko, S. K., Ksenofontov, D. A., Melchakova, L. V., and Ogorodova, L. P.: As-bearing phosphosiderite from Copiapo District, Atacama, Chile, Geochem. Int., 60, 1029–1032, 2022.

Huang, X.-L. and Shenker, M.: Water-soluble and solid-state speciation of phosphorus in stabilized sewage sludge, J. Environ. Qual., 33, 1895–903, 2004.

Kloprogge, T. and Wood, B. J.: X-ray photoelectron spectroscopic and Raman microscopic investigation of the variscite group minerals: Variscite, strengite, scorodite and mansfieldite, Spectrochim. Acta A, 185, 163–172, 2017.

Kniep, R. and Mootz, D.: Metavariscite – A redetermination of its crystal structure, Acta Crystallogr. B, 29, 2292–2294, 1973.

Knops-Gerrits, P.-P., Toufar, H., Li, X.-Y., Grobet, P., Schoonheydt, R. A., Jacobs, P. A., and Goddard III, W. A.: The structure of water in crystalline aluminophosphates: isolated water and intermolecular clusters probed by Raman spectroscopy, NMR and structural modeling, J. Phys. Chem. A, 104, 2410–2422, 2000.

Kolitsch, U., Weil, M., Kovrugin, V. M., and Krivovichev, S. V.: Crystal chemistry of the variscite and metavariscite groups: Crystal structures of synthetic $CrAsO_4 \cdot 2H_2O$, $TlPO_4 \cdot 2H_2O$, $MnSeO_4 \cdot 2H_2O$, $CdSeO_4 \cdot 2H_2O$ and natural bonacinaite, $ScAsO_4 \cdot 2H_2O$, Mineral. Mag., 84, 568–583, 2020.

Komissarova, L. N., Pushkina, G. Y., and Khrameeva, N. P.: Preparation and some properties of scandium arsenate dihydrate, Zh. Neorg. Khim., 16, 1538–1541, 1971 (in Russian).

Komissarova, L. N., Pushkina, G. Y., Khrameeva, N. P., and Teterin, E. G.: Scandium arsenates, Zh. Neorg. Khim., 18, 2316–2323, 1973 (in Russian).

Ivanov-Emin, B. N., Korotaeva, L. G., Moskalenko, V. I., and Ezhov, A. I.: Scandium arsenates, Zh. Neorg. Khim., 16, 2925–2928, 1971 (in Russian).

Lamoso, I. S. M. and Atencio, D.: Zoned phosphosiderite-metavariscite crystals from Eduardo Mine, Conselheiro Pena, Minas Gerais, Brazil, Geologia USP – Serie Cientifica, 17, 23–27, 2017.

Larsen, E. S. and Schaller, W. T.: The identity of variscite and peganite and the dimorphous form, metavariscite, Am. Mineral., 10, 23–28, 1925.

Larson, A. C. and Von Dreele, R. B.: General Structure Analysis System (GSAS), Los Alamos National Laboratory Report LAUR, 86–748, 1994.

Le Berre, J.-F., Gauvin, R., and Demopoulos, G. P.: Synthesis, structure, and stability of gallium arsenate dihydrate, indium arsenate dihydrate, and lanthanum arsenate, Ind. Eng. Chem. Res., 46, 7875–7882, 2007.

Loiseau, T., Paulet, C., and Férey, G.: Crystal structure determination of the hydrated gallium phosphate $GaPO_4 \cdot 2H_2O$, analog of variscite, C.R. Acad. Sci. II C, 1, 667–674, 1998.

Momma, K. and Izumi, F.: VESTA 3 for three-dimensional visualization of crystal, volumetric and morphology data, J. Appl. Crystallogr., 44, 1272–1276, 2011.

Mooney-Slater, R. C. L.: X-ray diffraction study of indium phosphate dihydrate and isostructural thallic compounds, Acta Crystallogr., 14, 1140–1146, 1961.

Mooney-Slater, R. C. L.: The crystal structure of hydrated gallium phosphate of composition $GaPO_4 \cdot 2H_2O$, Acta Crystallogr., 20, 526–534, 1966.

Moore, P. B.: The crystal structure of metastrengite and its relationship to strengite and phosphophyllite, Am. Mineral., 51, 168–176, 1966.

Oberti, R., Boiocchi, M., Hawthorne, F. C., and Ciriotti, M. E.: Magnesio-riebeckite from the Varenche mine (Aosta Valley, Italy): crystal-chemical characterization of a grandfathered end-member, Mineral. Mag., 81, 1431–1437, 2017.

O'Day, P. A.: Chemistry and Mineralogy of Arsenic, Elements, 2, 77–83, 2006.

Pasero, M., Reinecke, T., and Fransolet, A.-M.: Crystal structure refinements and compositional control of Mn-Mg-Ca ardennites from the Belgian Ardennes, Greece and the Western Alps, Neues Jb. Miner. Abh., 166, 137–167, 1994.

Pelloux, A.: Miniere e minerali manganesiferi della Valle d'Aosta, Rendiconti dei lavori dell'Ufficio Invenzioni e Ricerche – Giacimenti italiani di minerali accessori per la siderurgia, 1, 22–38, 1922 (in Italian).

Sabatini, A., Dapporto, P., and Bedini, E.: Tavola periodica e proprietà degli elementi (IUPAC), Edizioni Idelson Gnocchi, Napoli, Italy, 2017 (in Italian).

Schindler, M., Joswig, W., and Baur, W. H.: Preparation and crystal structures of the vanadium phosphates $VPO_4 \cdot 2H_2O$ and $V_{5.12}(PO_4)_4(OH)_{3.36}(H_2O)_{0.64} \cdot 0.84H_2O$, Eur. J. Sol. State Inor., 32, 109–120, 1995.

Sergeeva, A. V.: To the question of variscite and metavariscite formation, phase equilibria in the system $Al_2O_3 - H_2O - P_2O_5$. Zapiski RMO, 145, 101–113, 2016 (in Russian).

Sheldrick, G. M.: A short history of *SHELX*, Acta Crystallogr. A, 64, 112–122, 2008.

Siegfried, P., Wall, F., and Moore, K.: In search of the forgotten rare earth, Geoscientist, 28, 10–15, 2018.

Smith, D. G. W. and Nickel, E. H.: A system for codification for unnamed minerals: report of the Subcommittee for Unnamed Minerals of the IMA Commission on New Minerals, Nomenclature and Classification, Can. Mineral., 45, 983–1055, 2007.

Song, Y., Zavalij, P. Y., Suzuki, M., and Whittingham, M. S.: New iron(III) phosphate phases: crystal structure and electrochemical and magnetic properties, Inorg. Chem., 41, 5778–5786, 2002.

Spencer, E. C., Soghomonian, V., and Ross, N. L.: Gallium arsenate dihydrate under pressure: elastic properties, compression mechanism, and hydrogen bonding, Inorg. Chem., 54, 7548–7554, 2015.

Sugiyama, K., Yu, J., Hiraga, K., and Terasaki, O.: Monoclinic $InPO_4 \cdot 2H_2O$, Acta Crystallogr. C, 55, 279–281, 1999.

Tang, X., Gentiletti, M. J., and Lachgar, A.: Synthesis and crystal structure of indium arsenate and phosphate dihydrates with variscite and metavariscite structure types, J. Chem. Crystallogr., 31, 45–50, 2002.

Taxer, K. and Bartl, H.: On the dimorphy between the variscite and clinovariscite group: refined finestructural relationship of strengite and clinostrengite, $Fe(PO_4) \cdot 2H_2O$, Cryst. Res. Technol., 39, 1080–1088, 2004.

Warr, L. N.: IMA-CNMNC approved mineral symbols, Mineral. Mag., 85, 291–320, 2021.

Yang, H., Li, C., Jenkins, R. A., Downs, R. T., and Costin, G.: Kolbeckite, $ScPO_4 \cdot 2H_2O$, isomorphous with metavariscite, Acta Crystallogr. C, 63, i91–i92, 2004.

Yang, H., Li, C., Jenkins, R. A., Downs, R. T., and Costin, G.: Kolbeckite, $ScPO_4 \cdot 2H_2O$, isomorphous with metavariscite, Acta Crystallogr. C, 63, i91–i92, 2007.